0888-8809/07/$15.00/0
Printed in U.S.A.

Molecular Endocrinology 21(11):2750–2763

doi: 10.1210/me.2007-0263

Response of Candidate Sex-Determining Genes to Changes in Temperature Reveals Their Involvement in the Molecular Network Underlying Temperature-Dependent Sex Determination

Christina M. Shoemaker, Joanna Queen, and David Crews

Section of Integrative Biology, University of Texas at Austin, Austin, Texas 78712

Gonadogenesis, the process of forming an ovary or a testis from a bipotential gonad, is critical to the development of sexually reproducing adults. Although the molecular pathway underlying vertebrate gonadogenesis is well characterized in organisms exhibiting genotypic sex determination, it is less well understood in vertebrates whose sex is determined by environmental factors. We examine the response of six candidate sex-determining genes to sex-reversing temperature shifts in a species with temperature-dependent sex determination (TSD). For the first time, we report the regulation of *FoxL2*, *Wnt4*, *Dmrt1*, and *Mis* by temperature, confirming their involvement in the molecular pathway underlying TSD and placing them downstream of the action of temperature. We find evidence that *FoxL2* plays an ovarian-specific role in development, whereas *Wnt4* appears to be involved in both testis and ovary formation. *Dmrt1* expression shows rapid activation in response to a shift to male-producing temperature, whereas *Mis* up-regulation is delayed. Furthermore, early repression of *Mis* appears critical to ovarian development. We also investigate *Dax1* and *Sox9* and reveal that at the level of gene expression, response to temperature is comparatively later in gonadogenesis. By examining the role of these genes in TSD, we can begin to elucidate elements of conservation and divergence between sex-determining mechanisms. (*Molecular Endocrinology* 21: 2750–2763, 2007)

MANY VERTEBRATES EXHIBIT genotypic sex determination (GSD), in which a genetic factor determines the sexual fate of the initially bipotential gonad, as is the case in mammals via *Sry*. In other vertebrates, environmental factors dictate sexual fate. In temperature-dependent sex determination (TSD), the temperature at which the egg incubates during the middle third of embryonic development determines the future sex of the embryo. All crocodilians and many turtles and lizards exhibit TSD. Although the initial upstream factor determining sex differs between these modes, many of the downstream genes involved in the formation of the gonad may be retained.

Genes involved in GSD vertebrate gonadogenesis include *FoxL2*, *Wnt4*, *Dax1*, *Dmrt1*, and *Mis*. While the expression of some of these factors has been examined in organisms with TSD (1–9), their ability to respond to changes in temperature has not been investigated. Although experiments at constant incubation temperatures can correlate temporal and spatial patterns of gene expression to sexual fate, sex-reversing temperature-shift experiments represent an important functional manipulation in an organism lacking typical genetic techniques. Rapid change in gonadal expression of these genes after a temperature shift confirms a role in the formation of the gonad, whereas the timing of this response provides an indication of its hierarchical placement within the molecular cascade governing organ development. In this study, we examine the ability of temperature to regulate the expression of *FoxL2*, *Wnt4*, *Dax1*, *Dmrt1*, and *Mis*. The regulation of *Sox9* by temperature was demonstrated previously, and here we extend those results (10).

We examined the molecular pathway underlying TSD in the red-eared slider turtle, *Trachemys scripta*, a species that exhibits TSD. The slider turtle is sensitive to the effect of temperature from approximately Greenbaum's stage 14 through stage 19 at a female-producing temperature (FPT) and through stage 20 at a male-producing temperature (MPT) (11, 12). Cooler incubation temperatures (25–27 C) produce all male hatchlings and warmer temperatures (31–35 C) result in all female hatchlings, with varying sex ratios produced by temperatures in between (11, 13). Shifting eggs during the tempera-

First Published Online August 7, 2007

Abbreviations: AKG, Adrenal-kidney-gonad; DIG, digoxigenin; FPT, female-producing temperature; GSD, genotypic sex determination; HSD, honestly significant difference; MNE, mean normalized expression; MPT, male-producing temperature; qPCR, quantitative real-time RT-PCR; SSC, standard saline citrate; TSD, temperature-dependent sex determination; TSP, temperature-sensitive period.

***Molecular Endocrinology* is published monthly by The Endocrine Society (http://www.endo-society.org), the foremost professional society serving the endocrine community.**

ture-sensitive period (TSP) from one end of the temperature spectrum to the other (*i.e.* from 26 C to 31 C or *vice versa*) redirects gonadal development, resulting in 100% sex reversal (14–16).

The process of forming an ovary is less well understood than testicular differentiation (for review, see Ref. 17). Ovarian development is characterized by a proliferation of cells in the gonad's cortical region concurrent with medullary regression. Within the thickened cortex, granulosa cells organize to surround germ cells, whereas steroidogenic theca cells remain interstitial between developing follicles. One of the few ovarian-specific factors is *FoxL2* (*Forkhead box protein L2*), a single-exon transcription factor with a conserved winged-helix forkhead domain, mutations in which cause ovarian failure in humans with blepharophimosis/ptosis/epicanthus inversus syndrome (BPES) type I disease (18, 19). *FoxL2* is expressed in the developing ovary of mouse and chick embryos (7, 20) and is involved in postnatal mammalian granulosa cell differentiation (21). Furthermore, *FoxL2*−/− XX adult mice exhibit marked up-regulation of several testis-specific markers, including *Sox9*, *Dhh*, and *Fgf9*, indicating that *FoxL2* repression of testis-determining genes may occur well past mammalian embryonic sex determination (22). In *T. scripta*, *FoxL2* expression is detected in both MPT and FPT gonads and is later restricted to the developing ovary (7).

Wnt4 (*wingless-type MMTV integration site family member 4*) signaling has been implicated in the development of the vertebrate reproductive system in both sexes (see Ref. 23), mediating the initial formation of the Müllerian ducts and regulating the migration of steroidogenic mesonephric cells into the developing gonad (24, 25). In the ovary, *Wnt4* acts via *Follistatin* to prevent the formation of a testis-specific coelomic blood vessel (26). In *Wnt4*−/− XY mice, gonadal expression of *Sox9*, *Mis*, *Dhh*, and *Sf1* is decreased but can be rescued by ectopic Wnt4, suggesting an active role for *Wnt4* in testicular development as well (27). To our knowledge, the gene expression patterns or functional role of *Wnt4* has not been examined in an organism with TSD.

Dax1 (*Dosage-sensitive sex-reversal, Adrenal hypoplasia congenital on the X chromosome 1*, also known as *Nr0b1* and *Ahch*) is a novel orphan member of the nuclear hormone receptor superfamily and plays a role in both mammalian sex determination and adrenal function (see 28). Its early ovary- and late testis-specific expression pattern in the mouse suggests a complex role in the development of the gonad in both sexes (29). Similarly, it is expressed in both sexes in chick and two species with TSD, the American alligator and the Olive Ridley sea turtle (2, 5, 6). Originally thought to have an ovarian-determining function (30, 31), undisrupted embryonic gonadogenesis but abnormal postnatal formation of follicles in *Dax1*−/− XX mice led to the suggestion of an adult *Dax1* role in the ovary (32). In testicular development, *Dax1* may control availability of estrogens by regulating *aromatase* transcription (33–35). Furthermore, studies in mouse suggest that *Dax1* may be up-regulated by *Wnt4* signaling (36, 37).

The development of the vertebrate testis has been well studied and requires the action of *Dmrt1*, *Mis*, and *Sox9*, among other factors (for review, see Ref. 38). Elimination of *Dmrt1* (*Doublesex mab3-related transcription factor 1*) is thought to be responsible for male-to-female sex reversal seen in XY humans with chromosome 9 deletions (39). Although it seems to play a downstream role in testis differentiation in mammals (40), it has been proposed to be a master sex-determining gene in both chicken and medaka (41, 42). Extensive studies in mouse of the *Sry*-related gene *Sox9* (*SRY-like HMG-box 9*) have shown it to be both necessary and sufficient to cause the determination and differentiation of a testis (43). In both humans and mice, SOX9 interacts directly with SF1 (*Steroidogenic factor 1*) to up-regulate the expression of *Müllerian-inhibiting substance* (*Mis* or *anti-Müllerian hormone*, *Amh*) (44, 45). *Mis*, a member of the TGF-β superfamily, is one of the early factors secreted by differentiated Sertoli cells in the testis and causes the regression of the Müllerian ducts, anlagen that otherwise develop into the uterus, cervix, and fallopian tubes in females (46).

To identify possible roles in an organism with TSD, we report cloning *Wnt4* and *Dax1* in the red-eared slider turtle. We analyze the expression patterns of these two genes as well as *FoxL2* throughout six stages of gonadogenesis encompassing the temperature-sensitive sex-determining period. To examine the early factors directing a bipotential gonad down an ovary or a testis developmental trajectory, we extend our previous findings on the expression patterns of three testis-specific factors, *Dmrt1, Mis*, and *Sox9* to earlier time points within the TSP. To investigate placement of these factors in a temporal hierarchy regulating the development of the turtle gonad, we analyze their ability to rapidly respond to a shift in temperature during the sex-determining period. For the first time, we report a response of *FoxL2, Wnt4, Dmrt1*, and *Mis* to a change in temperature, confirming their role in the molecular pathway underlying TSD. As well, we provide evidence that *Dax1* is involved in gonadogenesis in both sexes, and we extend previous findings on the expression of *Sox9* in a species with TSD.

RESULTS

To investigate the role of genes possibly involved in sex determination and differentiation in an organism with TSD, we cloned *Wnt4* and *Dax1* in the red-eared slider turtle. We examine the spatial expression patterns of these genes, as well as *FoxL2*, at six stages of gonadogenesis by *in situ* hybridization on adjacent

gonad sections from five embryos. We analyzed expression levels of these three genes, as well as *Dmrt1, Mis*, and *Sox9,* at the same six stages of development as well as in response to sex-reversing temperature shifts, by quantitative real-time RT-PCR (qPCR) in three independent samples. All genes were found to have highly significant temperature by stage interaction effects (two-factor ANOVA, $P < 0.009$ for all genes, see supplemental Table 1, published as supplemental data on The Endocrine Society's Journals Online web site at http://mend.endojournals.org). *Post hoc* comparisons made between temperatures within each stage are described in this study for all genes except *Dax1*, which does not show a significant effect of temperature and is therefore analyzed within temperature between stages (see supplemental Tables 2 and 3, published as supplemental data on The Endocrine Society's Journals Online web site at http://mend.endojournals.org).

Examining a New Stage of Development

The TSP in *T. scripta* lasts from approximately stage 14 through stage 20, and shifting embryos between constant temperatures (26 and 31 C) during this time causes complete sex reversal (11). We used this lability to assess the involvement of various candidate genes in TSD gonadogenesis. After development progressed along one trajectory (MPT or FPT) for several stages during the sex-determining period, eggs were shifted at stage 16 to the opposite temperature. We assessed the ability of six candidate sex-determining genes to rapidly respond to this change in temperature at two subsequent time points. Turtle embryonic development is prolonged, and the period from stage 16 to stage 17 can last up to 2 d at FPT (31 C) or 4 d at MPT (26 C). Therefore, to examine the effects of the temperature shift on a finer temporal scale, we define a stage halfway between stage 16 and stage 17, termed stage 16.5. We distinguish this stage as having morphological characteristics midway between those associated with stages 16 and 17, as described in Fig. 1.

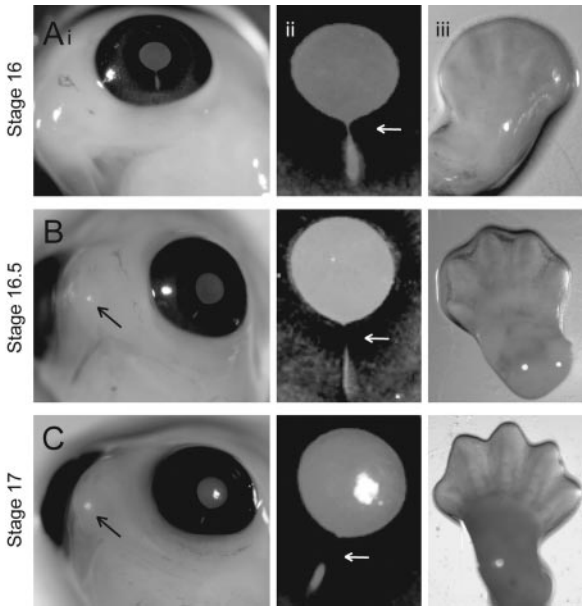

Fig. 1. Morphological Development of *T. scripta* during the TSP

A, Slider turtle stage 16 embryos exhibit i) smooth tissue on the upper jaw with no indication of caruncle, ii) a vertical line of unpigmented cells in the eye extending through the pupil (*white arrow*), and iii) large paddles with a smooth periphery and indications of digital ridges (12); B, to examine development on a finer time scale, we define stage 16.5 as having a small but visible caruncle, often still below the epidermal surface (*black arrow*), a diminished eyeline (*white arrow*), and slight indications of serrations along the paddle edge; C, by stage 17, a distinct white caruncle is found on the ventral surface of the upper jaw (*black arrow*), the vertical white line in the eye is substantially interrupted or absent (*white arrow*), and the edges of the paddle are clearly serrated.

FoxL2 Expression Becomes Ovarian Specific at the End of the TSP

In situ hybridization on sectioned adrenal-kidney-gonad (AKG) complexes reveals early *FoxL2* expression throughout the bipotential gonad developing at either temperature (stage 17, Fig. 2, A and B). At the end of the TSP, the spatial expression pattern of *FoxL2* in the developing ovary is localized primarily to the cortical region, although faint expression is seen in primitive sex cords that later degenerate (stage 19, Fig. 2C). Cortical expression in the ovary continues through differentiation (stage 23, Fig. 2E). Expression is also seen faintly at MPT at the close of the TSP and through differentiation in putative testicular seminiferous tubules (stages 19 and 23, Fig. 2, D and F). At all stages examined, *FoxL2* expression was detected in both sexes in the dorsal metanephric tubules of the future kidney, although more strongly at FPT (Fig. 2, G and H). Furthermore, expression of *FoxL2* occurs in epithelial cells lining the interior of the developing Müllerian duct of embryos at stages 19 and 23 (Fig. 2I, data not shown).

Expression levels of *FoxL2* measured by qPCR are similar between gonads developing at FPT and MPT early in the TSP (stages 16, 16.5, and 17, Fig. 3A). However, at the end of the TSP and through ovarian differentiation, FPT expression levels rise significantly above levels at MPT (stages 19, 21, and 23, $P < 0.0015$, Fig. 3A). Temperature-shifting embryos at stage 16 causes gonadal expression of *FoxL2* to rise, regardless of the direction of the shift (MPT→FPT or FPT→MPT, Fig. 3A′). However, this rise was significant in only one comparison: *FoxL2* expression in stage 16.5 MPT→FPT-shifted gonads is significantly higher than expression in unshifted stage 16.5 MPT gonads ($P < 0.009$, Fig. 3A′).

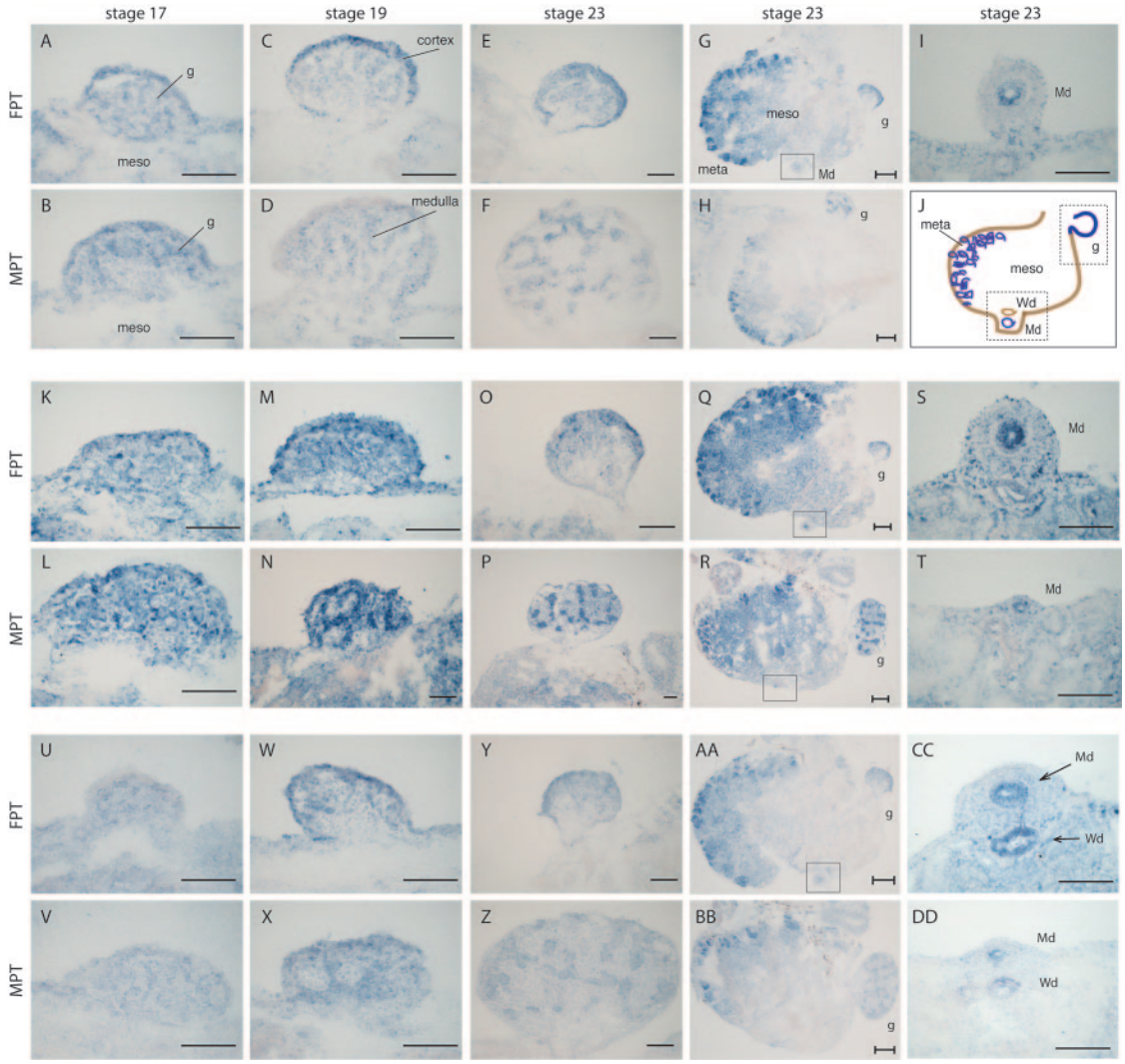

Fig. 2. Expression of *FoxL2, Wnt4*, and *Dax1* in the Turtle AKG Complex by *in Situ* Hybridization

A and B, *FoxL2* mRNA is found throughout bipotential gonads developing at both FPT and MPT; C and D, during the end of the TSP, expression at FPT begins to be localized in the cortex, whereas expression in both sexes is seen in primitive sex cords; E and F, by gonad differentiation, expression is concentrated cortically at FPT and seen faintly in putative sex cords at MPT; G and H, view of AKG reveals dorsal metanephric expression of *FoxL2* at both FPT and MPT; I, epithelial cells lining the interior of the Müllerian ducts express *FoxL2* at FPT and MPT, typified here in a stage 23 FPT embryo; J, view of AKG seen in G, H, Q, R, AA, and BB, with *dashed boxes* indicating views of gonad sections seen in A–F, K–P, and U–Z and of Müllerian and Wolffian duct sections seen in I, S, T, CC, and DD; K and L, *Wnt4* mRNA is found throughout bipotential gonads developing at both FPT and MPT during the TSP; M and N, by the end of the TSP, expression begins to localize in the cortex at FPT and in striped medullary patterns at MPT; O and P, through gonadal differentiation, expression becomes further localized to the ovarian cortical region and in putative testicular sex cords; Q and R, dorsal metanephric tissue strongly expresses *Wnt4* at both FPT and MPT, as does the mesonephros (*box* indicates Müllerian duct); S and T, epithelial cells lining the interior of the Müllerian ducts express *Wnt4* in both sexes; U–X, *Dax1* mRNA is found throughout gonads developing at both FPT and MPT during the TSP, loosely organized in the primitive sex cords that develop in both sexes; Y and Z, during gonadal differentiation, expression is localized to the cortical region at FPT and seen faintly at MPT; AA and BB, dorsal metanephric tissue also expresses *Dax1* at both FPT and MPT; CC and DD, epithelial cells of both the Müllerian and Wolffian ducts express *Dax1*. *Bar*, 100 μm; *bar with endcaps*, 200 μm. g, Gonad; Md, Müllerian duct; meso, mesonephros; meta, metanephros; Wd, Wolffian duct.

Wnt4 Is Widely Expressed throughout the Gonad, Mesonephros, and Metanephros

A partial homolog of *Wnt4* was cloned from turtle cDNA resulting in a 390-bp fragment. BLAST analysis indicated 85% nucleotide sequence homology to *Wnt4* in *Homo sapiens*, *Gallus gallus*, and *Mus musculus*. The putative translation deduced by MacVector software (MacVector, Inc., Cary, NC) is 129 amino acids long, corresponds to the coding region of exons 3 and 4 and the beginning of exon 5 of the mammalian protein (see supplemental Figs. 1 and 2, published as supplemental data on The Endo-

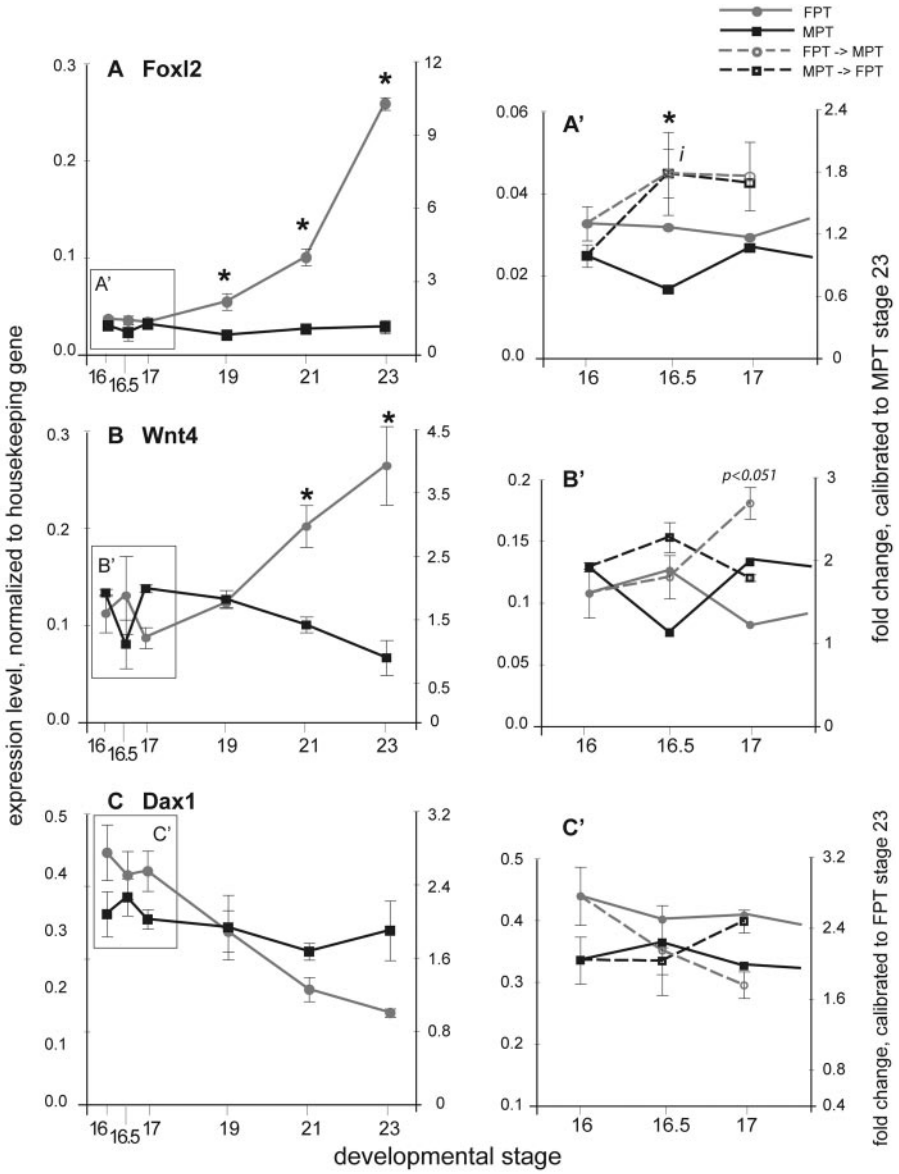

Fig. 3. Expression of *FoxL2*, *Wnt4*, and *Dax1* in the Turtle Gonad by qPCR

Expression levels were examined by qPCR in three samples per sex/stage, where each sample consisted of total RNA extracted from pooled gonads from 12–20 individuals. Average values are given with SE *bars*. *Left* y-axis indicates expression levels normalized to the housekeeping gene *PP1*, which is constitutively expressed across development. *Right* y-axis indicates fold change in normalized expression calibrated to the lowest expression value at stage 23, either MPT (*FoxL2*, *Wnt4*) or FPT (*Dax1*). *Asterisks* indicate statistically significant difference in expression between sex within stage at the $P = 0.05$ significance level, after correction for multiple pair-wise comparison tests by Tukey's HSD. A–C, Gene expression was examined at six stages through sex determination and differentiation at both MPT and FPT; A′–C′, expression data at MPT and FPT at three early stages during the TSP is expanded and compared with the response of gene expression to a shift in temperature. Embryos were shifted at stage 16 from either MPT to FPT (MPT→FPT) or FPT to MPT (FPT→MPT) and gonads dissected for analysis at two subsequent time points, stage 16.5 and stage 17. A′, *FoxL2* expression in MPT→FPT stage 16.5 gonads is significantly different from MPT stage 16.5 gonads, indicated by *i*, but is not different from other values at stage 16.5; B′, *Wnt4* expression in FPT→MPT stage 17 gonads is almost significantly different from expression in unshifted FPT stage 17 gonads ($P = 0.0508$); C′, *Dax1* expression is not significantly different in response to a temperature shift, although the direction of expression changes occurs in a sex-typical manner.

crine Society's Journals Online web site at http://mend.endojournals.org) and is 97% homologous to *H. sapiens*, 97% to *M. musculus*, and 95% to *G. gallus* Wnt4 amino acid sequence.

In situ hybridization detected *Wnt4* mRNA throughout the bipotential gonad during the TSP (stages 17 and 19, Fig. 2, K–N). This expression becomes primarily localized to the cortical region of the ovary and the

seminiferous tubules of the testis during gonad differentiation and is also retained between sex cords in the testis (stage 23, Fig. 2, O and P). At all stages examined, strong *Wnt4* expression in both sexes is observed in the mesonephros and dorsal metanephric tissues destined to become the adult kidney (Fig. 2, Q and R). Expression in the developing Müllerian ducts is found at stages 19, 21, and 23 in both sexes; in FPT embryos, *Wnt4* expression increases as the duct grows, whereas at MPT, expression decreases with duct regression (Fig. 2, S and T).

Throughout the TSP, *Wnt4* is expressed at comparable levels as measured by qPCR between gonads developing at FPT and MPT (stages 16–19, Fig. 3B). However, during ovarian differentiation, expression at FPT significantly rises above MPT by up to 4-fold (stage 21, $P = 0.015$; stage 23, $P < 0.0001$; Fig. 3B). In response to a FPT→MPT temperature shift, expression levels one stage later (stage 17) are increased from unshifted stage 17 FPT levels, although not significantly ($P = 0.0508$, Fig. 3B′). In gonads from the converse shift (MPT→FPT), *Wnt4* expression is not significantly different from unshifted levels at either time point.

Dax1 Is Expressed throughout the Gonad and Müllerian and Wolffian Ducts

To examine its expression in the slider turtle, we cloned a 297-bp fragment of *Dax1*. BLAST analysis identified 96% nucleotide sequence homology to *Dax1* in *Lepidochelys olivacae*, 92% to *Alligator mississippiensis*, 87% to *G. gallus*, and 78% homology to *H. sapiens*. The translated 98-amino-acid sequence (MacVector) corresponds to the C-terminal ligand-binding domain of the consensus vertebrate protein (see supplemental Figs. 3 and 4, published as supplemental data on The Endocrine Society's Journals Online web site at http://mend.endojournals.org) and is 95% homologous to *L. olivacea*, 93% to *A. mississippiensis*, 92% to *G. gallus*, and 76% to *H. sapiens* Dax1.

In situ hybridization during the TSP reveals a diffuse pattern of *Dax1* expression in gonads developing at FPT and MPT (stage 17, Fig. 2, U and V). At the end of the TSP, spatial expression patterns begin to organize (stage 19, Fig. 2, W and X), and during gonad differentiation, expression is concentrated in the cortex of ovaries and in a striped pattern indicative of sex cords in testes (stage 23, Fig. 2, Y and Z). At all stages examined, *Dax1* is expressed in dorsal metanephric tissue in both sexes, typified by the staining seen at stage 23 (Fig. 2, AA and BB). In both developing Müllerian and underlying Wolffian ducts, *Dax1* expression occurs in the epithelial cells lining the interior of the ducts (Fig. 2, CC and DD). Expression in Müllerian ducts is apparent at stages 19 (data not shown) and 23, whereas Wolffian duct expression is detected at stage 23. Some sections showed punctate *Dax1* expression in a mesonephric region from which adrenal tissue is expected to develop (data not shown).

Throughout gonadogenesis, *Dax1* expression levels measured by qPCR were not significantly different between gonads developing at MPT and FPT (Fig. 3C). However, within FPT, a significant change in expression between stages is observed. In the developing ovary, *Dax1* levels are significantly greater at stages 16, 16.5, and 17 than at stages 21 and 23 ($P < 0.009$ for all comparisons). In response to a shift in temperature, expression levels by stage 17 have changed in sex-typical directions, although not significantly (Fig. 3C′). Thus, after a MPT→FPT shift, *Dax1* expression levels are FPT-typical by stage 17, whereas after a FPT→MPT shift, they are MPT-typical.

Testis-Specific Genes Show a Rapid Response to Temperature Shifts

Previously, we examined the spatial and temporal expression patterns of *Dmrt1*, *Mis*, and *Sox9* throughout gonadogenesis in the slider turtle (9). Here, we report an extension of those results in three independent qPCR samples, reveal dimorphic expression levels earlier in the TSP than we previously described, and demonstrate that *Dmrt1* and *Mis* expression is regulated by temperature.

Beginning early in the TSP, expression of both *Dmrt1* and *Mis* is significantly higher at MPT as compared with FPT (*Dmrt1*: stage 16.5, $P < 0.027$, Fig. 4A; *Mis*: stage 16, $P < 0.007$, Fig. 4B). This pattern becomes substantially more dimorphic through testicular differentiation (stages 17, 19, 21, and 23, $P < 0.0001$ for both genes). In response to a FPT→MPT temperature shift, *Dmrt1* expression between stages 16.5 and 17 rises significantly above unshifted gonads remaining at FPT ($P = 0.0003$) and is not different from MPT expression levels (Fig. 4A′). Conversely, one stage after a MPT→FPT shift, expression levels have begun to drop but are not yet significantly lower than unshifted MPT levels. Thus, one stage after a temperature shift to MPT, expression of *Dmrt1* has been significantly up-regulated, but one stage after a shift to FPT, expression has not yet been significantly down-regulated (Fig. 4A′).

In contrast, *Mis* expression one stage after a MPT→FPT shift is significantly decreased from unshifted MPT levels ($P < 0.01$) and is not significantly different from FPT levels (stage 17, Fig. 4B′). After a FPT→MPT shift, expression has not significantly changed by stage 17 from unshifted FPT levels. Thus, expression of *Mis* has been significantly down-regulated one stage after a shift to FPT but has not yet been significantly up-regulated after a shift to MPT (Fig. 4B′).

Although *Dmrt1* and *Mis* show significantly dimorphic expression levels early in the TSP, *Sox9* expression levels are similar between gonads at MPT and FPT (stages 16, 16.5, and 17, Fig. 4C). *Sox9* expres-

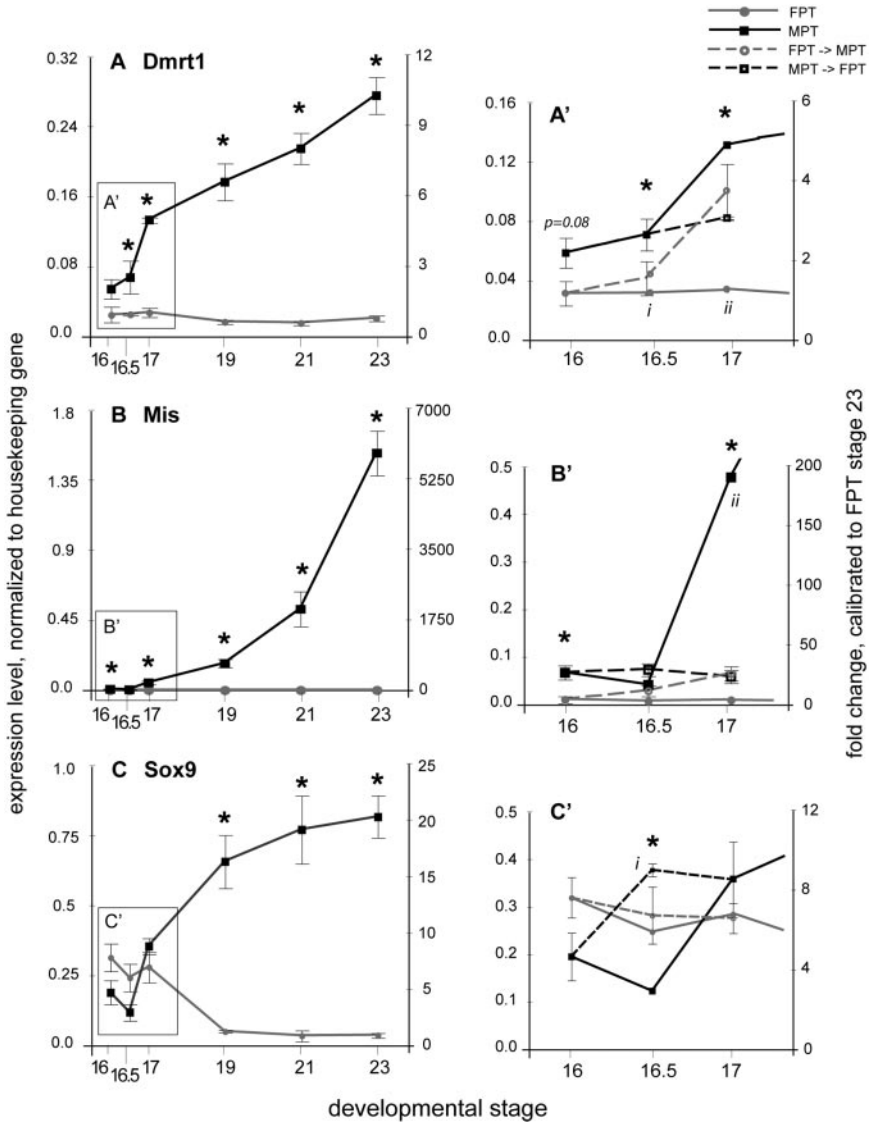

Fig. 4. Expression of *Dmrt1*, *Mis*, and *Sox9* in the Turtle Gonad by qPCR

Expression levels were examined by qPCR in three samples per sex/stage, where each sample consisted of total RNA extracted from pooled gonads from 12–20 individuals. Average values are given with SE *bars*. *Left* y-axis indicates expression levels normalized to the housekeeping gene *PP1*, which is constitutively expressed across development. *Right* y-axis indicates fold change in normalized expression calibrated to FPT stage 23. *Asterisks* indicate statistically significant difference in expression between sex within stage at the $P = 0.05$ significance level, after correction for multiple pair-wise comparison tests by Tukey's HSD. A–C, Gene expression was examined at six stages through development at both MPT and FPT; A′–C′, expression data at MPT and FPT at three early stages during the TSP is expanded and compared with the response of gene expression to a shift in temperature from either MPT to FPT or FPT to MPT. Embryos were shifted at stage 16 and gonads dissected for analysis at two subsequent time points, stage 16.5 and stage 17. A′, At stage 16.5, *Dmrt1* expression in FPT gonads is significantly lower than expression in both MPT and MPT→FPT gonads, indicated by *i*, and at stage 17, expression in FPT gonads is significantly lower than all three other measurements, indicated by *ii*; B′, at stage 17, *Mis* expression in MPT gonads is significantly higher than expression at all three other measurements, indicated by *ii*; C′, at stage 16.5, *Sox9* expression in MPT→FPT gonads is significantly higher than expression in MPT gonads, indicated by *i*.

sion in the putative turtle testis becomes significantly higher than in the developing ovary at the end of the sex-determining period (stage 19, $P < 0.0001$) and continues to be significantly higher through testicular differentiation (stages 21 and 23, $P < 0.0001$). Intriguingly, after a MPT→FPT shift, gonadal expression of *Sox9* increases significantly above unshifted MPT levels by one half-stage later (stage 16.5, $P < 0.006$) but are again indistinguishable from MPT by stage 17 (Fig. 4C′). After a FPT→MPT shift, expression is not different from unshifted FPT levels at either subsequent time point.

DISCUSSION

The molecular pathway underlying the formation of a testis and an ovary from a bipotential gonad has long been studied in organisms with genotypic sex-determining mechanisms. Although much of this pathway may be retained in organisms with other modes of sex determination, investigation of this has been slowed by a lack of functional manipulations in nonmodel organisms. Examining the response in the gonad of candidate sex-determining genes to changes in embryonic temperature allows a functional analysis of their involvement in the molecular pathway underlying gonadogenesis. Furthermore, the temporal order of expression changes triggered by sex-reversing temperature shifts may be used to infer the response to that environmental temperature regime under nonshift conditions. Thus, temperature-shift experiments provide insights into the relative hierarchical placement of gene action in this molecular cascade.

It should be noted that patterns of gene expression as analyzed by qPCR in this study reflect transcript abundance across the gonad as a whole and cannot take into account cell type differences in contribution to the total transcript pool. Germ cells and the various somatic cells that make up the gonad may be, and in fact are likely to be, expressing these gene products at different levels. Thus, if a temperature shift causes proliferation or loss of a particular cell type that is contributing to or causing an expression pattern, this subtlety may be lost in our analysis. Separating cell types of the gonad for quantitative analysis of gene expression would resolve this in future studies.

FoxL2 Expression Is Consistent with a Role in Ovarian Development

FoxL2 is one of the few ovarian-specific genes identified thus far, and a proposed function in mice is to repress male-specific gene expression postnatally (22). Although its expression in mouse during embryonic gonadogenesis is solely in the developing ovary, a sex-determining role during this period has not been identified. Here we confirm and extend a previous report of its expression pattern in *T. scripta* (7). *In situ* hybridization reveals localization of expression during differentiation in the cortex of the developing ovary, a pattern that is similar to other vertebrates. This pattern may reflect expression in the granulosa cell lineage, which is known to express *FoxL2* in mammals and localizes to the cortex, surrounding germ cells (22). Through quantitative real-time PCR, we are able to temporally define when expression at FPT significantly rises above MPT, which occurs at the close of the TSP. This pattern supports a role of *FoxL2* in ovarian development and suggests it may be involved in differentiation. Because expression is similar between the sexes early in the TSP, future temperature-shift experiments should extend past this period. However, regulation of *FoxL2* by temperature is observed, and taken together, our data provide evidence that *FoxL2* plays a role in the development of the ovary in an organism with TSD.

Although downstream target genes of *FoxL2* remain unknown, there is evidence for regulation of *aromatase* expression by *FoxL2* in chicken, trout, tilapia, and polled goats (47–50). *Aromatase* encodes the enzyme that converts androgens to estrogens. Hudson *et al.* (48) showed that inhibition of aromatase in the developing chick gonad leads to reduced, but not abolished, *FoxL2* expression. This is suggested to occur by a positive feedback mechanism in which *FoxL2* up-regulates *aromatase*, which then enhances *FoxL2* activation. Furthermore, it was recently shown by Ramsey *et al.* (51) that *T. scripta* gonadal *aromatase* expression is dimorphic between FPT and MPT embryos early in the TSP; expression at FPT is organized in circular clusters of expressing cells surrounding nonexpressing cells, putatively pregranulosa cells surrounding germ cells, whereas at MPT, expression remains unorganized. If a positive feedback loop exists between *FoxL2* and *aromatase* in an organism with TSD, exogenous aromatase inhibitor in turtle embryos should also cause decreased *FoxL2* expression.

Expression of *Wnt4* Is Conserved across GSD and TSD Vertebrates and Is Consistent with a Role in Both Ovary and Testis Development and Duct and Kidney Formation

To our knowledge, examination of *Wnt4* in the slider turtle represents the first analysis of this signaling molecule in an organism with TSD. Here we find *Wnt4* is expressed in turtle gonads developing at both MPT and FPT throughout the periods of sex determination and gonad differentiation, suggesting that it functions in both the developing testis and ovary. Expression at MPT begins to localize in a striped pattern indicative of developing sex cords as early as the end of the TSP, although expression in interstitial cells between cords is retained. Expression in the ovary becomes concentrated in the cortical region, and during differentiation, quantitative real-time PCR shows expression levels at FPT rise significantly above MPT. It is possible that this up-regulation reflects a shift in *Wnt4* function during gonad differentiation to a later female-specific role.

Mouse studies support a complex role for *Wnt4* in both male and female development, and the regulation of *Wnt4* signaling in a bipotential gonad presents an interesting problem. It was recently suggested that antagonistic action between *Wnt4* and *Fgf9* signaling pathways regulate the switch between ovarian and testicular development in the mammalian bipotential gonad (52). However, *Wnt4* may have several sex-specific roles throughout gonadogenesis. For example, *Wnt4*−/− XY mice retain normal *Sry* expression but have decreased levels of *Sox9* and *Dhh* expression, disrupted Sertoli cell differentiation, and a substantial overpopulation of steroidogenic cells migrat-

ing into the gonad from the mesonephros (27). Thus, an important role for *Wnt4* in the developing mammalian testis includes regulating the migration of these cells, whereas wholly preventing this migration into developing ovaries. The expression of *Wnt4* in the turtle in the mesonephros of both sexes as well as in developing sex cords and interstitial cells of the testis may reflect a similar role. Mesonephric expression of *Wnt4* is also important in the development of other vertebrate organs and is required for the cellular mesenchymal-to-epithelial transition that occurs during mammalian kidney tubule formation (53). Strong turtle *Wnt4* expression in developing mesonephric and metanephric tissues destined to become the kidney is consistent with a similar function in an organism with TSD.

A testis-specific medullary coelomic blood vessel forms during mammalian gonadogenesis. It was shown that *Wnt4*−/− XX mice ectopically develop this blood vessel, whereas overexpression of *Wnt4* in XY mice results in a disorganized coelomic blood vessel (25, 54, 55). If a similar coelomic blood vessel forms in MPT organisms with TSD, a possible role for *Wnt4* expression seen in the medullary region of the developing turtle ovary may be repressing its formation at FPT.

Finally, the role of *Wnt4* in the formation of the Müllerian ducts, anlagen that initially form in both sexes and then develop into the cervix, uterus, and oviducts in females, has been examined extensively in the mouse. It is suggested that *Wnt9b* up-regulates *Wnt4*, which leads to initial Müllerian duct formation in both sexes as well as inhibition of *Wnt7a* and *Pax8* (24, 53, 56). In males, *Mis* then causes the degradation of these ducts. Lack of either *Wnt9b* or *Wnt4* prevents the initial formation of Müllerian ducts, whereas a lack of *Wnt7a* results in persistent ducts and prevents downstream organs from forming (53, 56). In the turtle, the Müllerian duct develops in both sexes in a rostral to caudal wave and appears along the anterior/posterior axis near the gonad at the end of the TSP (stage 18/19) (57). Müllerian duct primordia develop in both sexes for two stages and then enlarge at FPT and degrade at MPT (57). Our data show that before Müllerian ducts form, *Wnt4* is expressed in the mesonephric tissue from which they will derive. Furthermore, *Wnt4* expression is detected within primordial Müllerian ducts from the first stage they appear. This early expression pattern is consistent with a role for *Wnt4* signaling in the embryonic development of these ducts.

Dax1 Expression Is Consistent with a Role in Gonad and Adrenal Development

The complexity of the role of *Dax1* in vertebrate sexual development has thus far prevented a clear understanding of its function. Expression is detected early in the development of the vertebrate gonad, and in mammals, this expression becomes female specific through time, whereas in chick, expression continues in both the testis and ovary (2, 31). To examine its role in an organism with TSD, we cloned a partial *Dax1* sequence in the slider turtle and find a similar expression pattern to chick. *Dax1* is gonadally expressed throughout sex determination and differentiation at levels that are not significantly different between MPT and FPT gonads, although expression at FPT does decrease significantly through time. Furthermore, *Dax1* mRNA first appears dispersed throughout the bipotential gonad and then becomes progressively restricted to the ovarian cortex and testicular sex cords. *Dax1* is involved in the formation of the human adrenal cortex (28, 58). Here we find *Dax1* expression in the turtle in a region of the mesonephros from which adrenal gland develops, indicating conservation of expression pattern. Interestingly, *Dax1* is the only gene examined in this study by *in situ* hybridization expressed in the developing Wolffian ducts, structures that eventually degrade in females and become functional tubules in males.

To explain its complex role in both developing mammalian testes and ovaries, a dosage-dependent mechanism has been proposed in which one copy of X-linked *Dax1* plays a role in activating male development, whereas two copies can inhibit *Sry* action (34, 35, 59). Because organisms with TSD are thought not to have functional sex chromosomes, dosage-dependent regulation in these systems could be conserved if regulated by a different mechanism. There are presumably two *Dax1* gene copies in every diploid turtle embryo, and thus functional *Dax1* differences must be regulated at transcriptional or translational levels. Furthermore, if the role of DAX1 is dose dependent, this regulation must at some point be correlated with incubation temperature. In this study, we find that expression levels between MPT and FPT are not significantly different, and consequently, any dimorphic DAX1 function must be posttranscriptionally regulated in the turtle. During the preparation of this manuscript, a model of dosage-dependent sex determination in organisms exhibiting TSD was proposed in which effects of a Z-linked male determinant depend on both temperature and copy number, and our data are not inconsistent with this mechanism (60).

A regulatory relationship between *Wnt4* and *Dax1* has been previously postulated, in which *Wnt4* signaling leads to activation of *Dax1* in a sex-specific manner (37). *Wnt4*−/− XX mice show decreased *Dax1* expression at 11.5 d postcoitum, whereas no change in expression level is observed in 11.5-d postcoitum *Wnt4*−/− XY mice (37). The general colocalization of expression of these factors in the developing turtle gonad is consistent with regulation of *Dax1* by *Wnt4* in an organism with TSD, and additional experiments are required to explore this possibility.

Response to Temperature Suggests an Early Role for *Dmrt1* and a Later Role for *Mis* in Testicular Development

As expected from our previous work (9), expression levels of *Dmrt1*, *Mis*, and *Sox9* are strongly sexually dimorphic during gonadogenesis. By quantitative real-time PCR, both *Dmrt1* and *Mis* are expressed at significantly higher levels at MPT as compared with FPT beginning early in the TSP. For both genes, these levels become increasingly disparate through differentiation. In contrast, *Sox9* is expressed in both sexes during the TSP and become significantly greater at MPT at the end of the TSP and during differentiation.

For the first time, we report a transcriptional response of *Dmrt1* and *Mis* to a shift in embryonic temperature. *Dmrt1* expression in the gonad shows a rapid response when embryos are shifted from FPT to MPT; between one half and one stage later, expression is up-regulated to a level significantly greater than unshifted FPT levels and is not different from MPT levels. The converse shift from MPT to FPT does not show a significant change one stage later, although *Dmrt1* expression has begun to drop toward FPT levels. Taken together, these data indicate that testicular development requires the rapid up-regulation of *Dmrt1* and places the action of *Dmrt1* downstream of temperature. Furthermore, it suggests an early role for *Dmrt1* function in the developing testis and an upstream position in the temporal hierarchy of genes underlying development of the gonad. Delayed response in gonads shifted toward FPT suggest that repression of this gene may be a later event in the molecular cascade governing ovarian development.

In contrast to the case with *Dmrt1*, *Mis* shows a different type of rapid response to temperature. After a shift from FPT to MPT, gonadal *Mis* expression one stage later has begun to increase but is not yet statistically higher than unshifted FPT levels. This suggests that the role of *Mis* is downstream of *Dmrt1* in the molecular hierarchy governing testicular development, given the assumption that *Mis* has not yet been up-regulated by upstream factors. Conversely, response of *Mis* expression to a shift from MPT to FPT shows a dramatic change one stage later. Expression is significantly down-regulated from unshifted MPT levels and is not distinguishable from FPT levels. One testis-specific function of *Mis* in mammals is to induce regression of the Müllerian ducts, which otherwise differentiate into female-specific organs. The repression of this hormone is thus critical in mammalian ovaries, and our data suggest the same may be true in organisms with TSD. The extremely low levels of *Mis* observed in FPT gonads at all stages, as well as the rapid down-regulation after a shift to an FPT, support this hypothesis.

Although the temporal response of gene expression to a temperature shift can be used to infer placement of gene action in the molecular hierarchy governing gonadogenesis, we cannot rule out the possibility that this response does not occur under constant conditions. Thus, it should be considered that a novel environmental temperature may not engender the same molecular response as in an embryo experiencing the same temperature in nonshift conditions.

Here we demonstrate that *Sox9* expression levels in the turtle gonad are statistically similar in both sexes early in the TSP. By qPCR, we temporally define when *Sox9* expression becomes significantly male specific, which occurs at the end of the TSP. However, as is true for any monomorphic gene expression pattern, SOX9 protein may be differentially functional at an earlier time point than when dimorphic expression occurs. It was shown that in response to a MPT→FPT temperature shift, SOX9 protein levels decreased in cultured gonad explants within the TSP (10). Furthermore, SOX9 remains cytoplasmic in cells of the mammalian bipotential XX gonad but is translocated to the nucleus in XY gonads where it can regulate downstream gene transcription (61, 62). Thus, although our quantitative expression data supports a later role for *Sox9* in the development of the testis, differential *Sox9* function may occur earlier via translational regulation of SOX9 or subcellular localization of the *Sox9* mRNA or protein.

Examining the patterns of up-regulation of these testicular genes may also reveal something about their role in development. *Dmrt1* and *Sox9* expression levels rise sharply early in development, showing the greatest activation in expression in the middle of the TSP, between stages 16 and 19. In contrast, *Mis* expression increases most dramatically at the end of the TSP and during differentiation, from stage 19 to stage 23, implying a later role and suggesting up-regulation by earlier testis-specific genes. A candidate for activating *Mis* is *Sox9*, because it is known to directly target *Mis* in mammals (44, 45). As discussed, differential SOX9 protein translation or localization provides a mechanism by which equal levels of *Sox9* expression could differentially regulate *Mis* activation in the turtle and, although not tested in the current study, warrants future attention.

In this study, we examine the spatial and temporal response of six candidate sex-determining genes to a sex-reversing change in temperature. This functional manipulation in a nonmodel system allows an analysis of their hierarchical placement within the molecular network governing gonadogenesis. By studying the molecular cascade regulating the development of a testis and an ovary from a bipotential gonad in an organism with TSD, we begin to identify components of the pathway that may be functionally conserved through diverse modes of sex determination.

MATERIALS AND METHODS

Collection and Harvesting of Embryos

Freshly laid red-eared slider eggs purchased from Clark Turtle Farms (Hammond, LA) were maintained as previously described (11), in accordance with humane animal practices under Institutional Animal Care and Use Committee protocol 03102301. Briefly, viable eggs were randomized in trays of moistened vermiculite and placed in incubators (Precision, Chicago, IL) at 26.0 or 31.0 C. Incubator temperatures were monitored daily with HOBO data loggers (Onset Computer Corp., Bourne, MA) and verified with calibrated thermometers. For temperature-shift experiments, multiple trays of 30 eggs per tray were shifted at developmental stage 16 from incubators held at 26.0 to 31.0 C and vice versa.

Staging

Progression of development was monitored by staging external morphological characteristics of a sampling of individuals according to Greenbaum's staging series (12). Morphological characteristics of a stage 16 slider turtle include the initial formation of a beak, a white line that extends ventrally from the pupil of the eye, and a large digital plate with a smooth periphery with slight indications of digital ridges (Fig. 1A). By stage 17, a white caruncle, or egg tooth, has formed on the upper jaw, the white line of the eye is absent or interrupted as pigmented cells reorganize, and the periphery of the digital plate is serrated with well-developed digital ridges (Fig. 1C). We defined stage 16.5 for the purposes of this study as midway between stages 16 and 17, characterized by a caruncle that is just visible and slightly below the epidermis of the beak, a narrowing white eye line, and slight serrations around the periphery of the digital plate (Fig. 1B). For morphological characteristics representative of other stages, see Greenbaum (12).

Cloning of Turtle Gene Homologs

Total RNA was extracted from pooled AKG complexes from a variety of sexes and stages and reverse-transcribed using oligo(dT) primers with Superscript II reverse transcriptase (Invitrogen, Carlsbad, CA). Primers for *Dax1* and *FoxL2* were designed based on published mouse, human, alligator, and chicken sequences where available and were *Dax1*, 5′-AGT GCT GGA GCC TGG ACA TCG-3′ and 5′-CAT CTC CAG CAG CAT GTC ATC C-3′, and *FoxL2*, 5′-TCC GGC ATC TAC CAG TA-3′ and 5′-TTG CCG GGC TGG AAG TG-3′. *Wnt4* primers amplifying a 390-bp fragment based on mammalian sequences were a gift from Pascal Bernard and were 5′-GTA CCT GGC CAA GCT GTC-3′ and 5′-AGC ATC CTG ACC ACT GGA AGC-3′. Amplified fragments were ligated into pCR4-TOPO vector according to the manufacturer's protocol (Invitrogen) and sequenced using M13F and M13R primers. The sequence of the 261-bp *FoxL2* clone was subsequently found to correspond to bp 73–330 of a previously published *T. scripta FoxL2* sequence (7) (accession no. AY155535). Sequences for *Dax1* and *Wnt4* were submitted to GenBank (accession nos. EF591056 and EF591055, respectively).

In Situ Hybridization

AKG complexes were dissected from embryos, immediately frozen in OCT embedding medium, and stored at −80 C. They were subsequently serially sectioned in four series on a 2800 Reichert-Jung cryostat at 20 μm and thaw-mounted onto SuperFrost Plus slides (Erie Sciientific Co., Portsmouth, NH). Sections were fixed in cold 4% paraformaldehyde, washed in PBS, and incubated in 0.25% acetic anhydride/triethanolamine. After washes in 2× standard saline citrate (SSC), slides were dehydrated in an increasing ethanol series, air dried, and stored at −80 C. Riboprobes were reverse-transcribed in the presence or absence of digoxigenin (DIG)-labeled UTP (Roche, Indianapolis, IN) using a T3/T7 Megascript *in vitro* transcription kit (Ambion, Austin, TX) to produce antisense or sense DIG-labeled or unlabeled riboprobes. Slides were warmed to room temperature, air dried, and preequilibrated in hybridization buffer (50% formamide, 5× SSC, 5× Denhardt's solution, 125 μg/ml Baker's yeast tRNA, 250 μg/ml denatured herring sperm DNA) for 2 h at either 50 C (*Wnt4*, *FoxL2*) or 45 C (*Dax1*). Sections were incubated in riboprobe overnight at the same temperatures, respectively. Experimental slides were exposed to antisense DIG-labeled probe, whereas control slides were incubated in either sense DIG-labeled probe or a competitive series of antisense DIG-labeled/unlabeled probes. After RNase A treatment at 37 C, sections were washed in a decreasing series of SSC and equilibrated in 150 mM NaCl/100 mM Tris (pH 7.5) at room temperature before incubation in 1:5000 anti-DIG-alkaline phosphatase Fab fragments (Roche) in 0.5% Tween 20/PBS for 2 h at room temperature. Sections were washed in 100 mM Tris (pH 7.5) and incubated in 5 mM levamisole [in 100 mM Tris (pH 9.5), 100 mM NaCl, 50 mM $MgCl_2$ buffer]. Chromogenic product was formed using nitroblue tetrazolium/5-bromo-4-chloro-3-indolyl-phosphate chromogen in 100 mM Tris (pH 8.0) (Roche) at 30 C until desired darkness was achieved and was terminated simultaneously for all slides within a gene. Sections were dehydrated, delipidated, and coverslipped under Permount (Fisher). Sets of gonads from five embryos per sex/stage were analyzed.

qPCR

Embryos were removed from the egg, staged, and killed by rapid decapitation. AKG complexes were immediately dissected and floated in sterile PBS. Pairs of gonads were cut away from underlying mesonephric tissues using fine scissors and a dissecting microscope from 12–20 embryos per independent sample (n = 3 at each sex/stage), pooled, immediately placed in RNA denaturing solution (Promega, Madison, WI), vortexed to dissociate, and stored at −80 C. A maximum of 5 min elapsed from decapitation to placement in denaturing solution. Total RNA was extracted using the RNAgents Total RNA Isolation kit (Promega) and treated with DNA-Free DNase I (Ambion, Austin, TX). cDNA was reverse-transcribed using the SuperScript First-Strand Synthesis for RT-PCR system (Invitrogen) with both oligo-(dT) and random hexamer primers. Relative gene expression levels were quantified using SYBR Green I dye (Invitrogen) and an ABI PRISM 7900HT real-time PCR cycler (ABI SDS 2.2.1 software). Samples were each run in triplicate, and the median value was used for analysis. PCR efficiencies were calculated from gene-specific standard curves. Relative transcript abundance was normalized to expression of *protein phosphatase 1* (*PP1*), a constitutively expressed transcript across both stage and sex selected previously (9). A modified ΔCT method that allows for correction of differential gene PCR efficiencies was used, where mean normalized expression (MNE) is calculated as follows: $MNE = \text{mean}\ [(E_{ref} - Ct_{ref})/(E_{target} - Ct_{target})]$, where E is gene-specific PCR efficiency, Ct is cycle threshold from each independent sample, target is gene of interest, and ref is constitutively expressed reference gene (63–65). To examine expression fold changes within a gene, MNE values were calibrated to the lower value at stage 23 (either MPT or FPT). Primers used to assay gene expression were designed across exon boundaries for *Wnt4* and *Dax1* using MacVector; this was not possible for *FoxL2*, which contains a single exon. Primer specificity was verified by agarose gel electrophoresis, and for *PP1*, *Dmrt1*, *Mis*, and

Sox9 were as previously described (9). qPCR primers for *FoxL2, Wnt4*, and *Dax1* were as follows: *FoxL2*, forward 5′-TGG CAG AAC AGC ATC CGC-3′ and reverse 5′-GGG TCC AGC GTC CAG TAG TTG-3′; *Wnt4*, forward 5′-CCG TAA CCG TCG CTG GAA C-3′ and reverse 5′-GGA GGA GAT GGC ATA CAC AAA AGC-3′; *Dax1*, forward 5′-GGA CTG TGC TCT TCA ACC CG-3′ and reverse 5′-GCT TGC TGT GCT TCC CTC TG-3′.

Stastical Analysis

For each gene, expression values measured by qPCR relative to the housekeeping gene (*PP1*) were plotted to test normality. *Wnt4* and *Dax1* data were found to have normal distributions, whereas *FoxL2*, *Dmrt1*, *Mis*, and *Sox9* values were log-transformed to meet the normality assumption. A two-factor ANOVA (mixed data) on all MNE values within a gene tested for sex, stage, and sex by stage interaction effects (SAS software program; SAS Institute, Inc., Cary, NC). *Post hoc* pairwise comparison tests of all possible comparisons within a gene were analyzed (every combination of two MNEs), correcting for multiple tests using Tukey's honestly significant difference (HSD).

Acknowledgments

We thank Pascal Bernard for the kind gift of *Wnt4* primers; Raymond Porter, Mary Ramsey, Kristen Berkstresser, Kyle Jackson, and Dr. James Skipper for technical contributions; Molly Cummings for generosity in using her equipment; Tom Juenger for help with statistical analysis; and Brian Dias and Nicholas Sanderson for helpful comments during manuscript preparation. We also thank reviewers from whom we received insightful editorial comments.

Received May 21, 2007. Accepted August 1, 2007.

Address all correspondence and requests for reprints to: David Crews, West 24th and Speedway, Patterson Labs, Austin, Texas 78705. E-mail: crews@mail.utexas.edu.

This work was funded by a National Science Foundation grant (IBN 200001269) to D.C. and a Graduate Research Fellowship from The University of Texas at Austin to C.S.

Disclosure Statement: The authors have nothing to disclose.

REFERENCES

1. Spotila LD, Spotila JR, Hall S 1998 Sequence and expression analysis of Wt1 and *Sox9* in the red-eared slider turtle, *Trachemys scripta*. J Exp Zool 281:417–427
2. Smith C, Smith M, Sinclair AH 1999 Gene expression during gonadogenesis in the chicken embryo. Gene 234: 395–402
3. Moreno-Mendoza N, Harley V, Merchant-Larios H 1999 Differential expression of SOX9 in gonads of the sea turtle *Lepidochelys olivacea* at male- or female-promoting temperatures. J Exp Zool 284:705–710
4. Western PS, Harry JL, Graves JA, Sinclair AH 1999 Temperature-dependent sex determination in the American alligator: *Amh* precedes *Sox9* expression. Dev Dyn 216: 411–419
5. Western PS, Harry JL, Marshall Graves JA, Sinclair AH 2000 Temperature-dependent sex determination in the American alligator: expression of SF1, WT1, and DAX1 during gonadogenesis. Gene 241:223–232
6. Torres-Maldonado L, Piedra AL, Moreno-Mendoza N, Valencia AM, Martinez AM, Merchant-Larios H 2002 Expression profiles of *Dax1*, *Dmrt1*, and *Sox9* during temperature sex determination in gonads of the sea turtle *Lepidochelys olivacea*. Gen Comp Endocrinol 129:20–26
7. Loffler KA, Zarkower D, Koopman P 2003 Etiology of ovarian failure in blepharophimosis ptosis epicanthus inversus syndrome: FOXL2 is a conserved, early-acting gene in vertebrate ovarian development. Endocrinology 144:3237–3243
8. Takada S, DiNapoli L, Capel B, Koopman P 2004 Sox8 is expressed at similar levels in gonads of both sexes during the sex determining period in turtles. Dev Dyn 231: 387–395
9. Shoemaker C, Ramsey M, Queen J, Crews D 2007 Expression of *Sox9*, *Mis* and *Dmrt1* in the gonad of a species with temperature-dependent sex determination. Dev Dyn 236:1055–1063
10. Moreno-Mendoza N, Harley VR, Merchant-Larios H 2001 Temperature regulates SOX9 expression in cultured gonads of *Lepidochelys olivacea*, a species with temperature sex determination. Dev Biol 229:319–326
11. Wibbels T, Bull JJ, Crews D 1991 Chronology and morphology of temperature-dependent sex determination. J Exp Zool 260:371–381
12. Greenbaum E 2002 A standardized series of embryonic stages for the emydid turtle *Trachemys scripta*. Canadian J Zool 80:1350–1370
13. Wibbels T, Bull JJ, Crews D 1994 Temperature-dependent sex determination: a mechanistic approach. J Exp Zool 270:71–78
14. Crews D, Bergeron JM, Bull JJ, Flores D, Tousignant A, Skipper JK, Wibbels T 1994 Temperature-dependent sex determination in reptiles: proximate mechanisms, ultimate outcomes, and practical applications. Dev Genet 15:297–312
15. Crews D 1996 Temperature-dependent sex determination: the interplay of steroid hormones and temperature. Zool Sci 13:1–13
16. Crews D 2003 Sex determination: where environment and genetics meet. Evol Dev 5:50–55
17. Yao HH 2005 The pathway to femaleness: current knowledge on embryonic development of the ovary. Mol Cell Endocrinol 230:87–93
18. Crisponi L, Deiana M, Loi A, Chiappe F, Uda M, Arnati P, Bisceglia L, Zelante L, Nagaraja R, Porcu S, Ristaldi MS, Marzella R, Rocchi M, Nicolino M, Lienhardt-Roussie A, Nivelon A, Verloes A, Schlessinger D, Gasparini P, Bonneau D, Cao A, Pilia G 2001 The putative forkhead transcription factor *FoxL2* is mutated in blepharophimosis/ptosis/epicanthus inversus syndrome. Nat Genet 27: 159–166
19. Udar N, Yellore V, Chalukya M, Yelchits S, Silva-Garcia R, Small K, BPES Consortium 2003 Comparative analysis of the *FoxL2* gene and characterization of mutations in BPES patients. Hum Mutat 22:222–228
20. Govoroun MS, Pannetier M, Pailhoux E, Cocquet J, Brillard JP, Couty I, Batellier F, Cotinot C 2004 Isolation of chicken homolog of the *FoxL2* gene and comparison of its expression patterns with those of aromatase during ovarian development. Dev Dyn 231:859–870
21. Schmidt K, Ovitt CE, Anlag K, Fehsenfeld S, Gredsted L, Treier AC, Treier M 2004 The murine winged helix transcription factor *FoxL2* is required for granulosa cell differentiation and ovary maintenance. Development 131: 933–942
22. Ottolenghi C, Omari S, Garcia-Ortiz JE, Uda M, Crisponi L, Forabosco A, Pilia G, Schlessinger D 2005 FoxL2 is required for commitment to ovary differentiation. Hum Mol Gen 14:2053–2062
23. Bernard P, Harley VR 2007 *Wnt4* action in gonadal development and sex determination. Int J Biochem Cell Biol 39:31–43

24. Vainio S, Heikkila M, Kispert A, Chin N, McMahon AP 1999 Female development in mammals is regulated by Wnt-4 signaling. Nature 397:405–409
25. Jeays-Ward K, Hoyle C, Brennan J, Dandonneau M, Alldus G, Capel B, Swain A 2003 Endothelial and steroidogenic cell migration are regulated by *Wnt4* in the developing mammalian gonad. Development 130: 3663–3670
26. Yao HHC, Matzuk MM, Jorgeq CJ, Menke DB, Page DC, Swain A, Capel B 2004 Follistatin operates downstream of *Wnt4* in mammalian ovary organogenesis. Dev Dyn 230:210–215
27. Jeays-Ward K, Dandonneau M, Swain A 2004 Wnt4 is required for proper male as well as female sexual development. Dev Biol 276:431–440
28. Niakan KK, McCabe ER 2005 DAX1 origin, function and novel role. Mol Genet Metab 86:70–83
29. Ikeda Y, Swain A, Weber TJ, Hentges KE, Zanaria E, Lalli E, Tamai KT, Sassone-Corsi P, Lovell-Badge R, Camerino G, Parker KL 1996 Steroidogenic factor 1 and Dax-1 colocalize in multiple cell lineages: potential links in endocrine development. Mol Endocrinol 10: 1261–1272
30. Bardoni B, Zanaria E, Guioli S, Floridia G, Worley K, Tonini G, Ferrante E, Chiumello G, McCabe E, Fraccaro M 1994 A dosage sensitive locus at chromosome Xp21 is involved in male to female sex reversal. Nat Genet 7:497–501
31. Swain A, Zanaria E, Hacker A, Lovell-Badge R, Camerino G 1996 Mouse *Dax1* expression is consistent with a role in sex determination as well as in adrenal and hypothalamus function. Nat Genet 12:404–409
32. Yu RN, Ito M, Saunders TL, Camper SA, Jameson JL 1998 Role of Ahch in gonadal development and gametogenesis. Nat Genet 20:353
33. Wang ZJ, Jeffs B, Ito M, Achermann JC, Yu RN, Hales DB, Jameson JL 2001 Aromatase (Cyp19) expression is upregulated by targeted disruption of *Dax1*. Proc Natl Acad Sci USA 98:7988–7993
34. Meeks JJ, Weiss J, Jameson JL 2003 Dax1 is required for testis determination. Nat Genet 34:32–33
35. Meeks JJ, Crawford SE, Russell TA, Morohashi K, Weiss J, Jameson JL 2003 Dax1 regulates testis cord organization during gonadal differentiation. Development 130: 1029–1036
36. Jordan BK, Mohammed M, Ching ST, Delot E, Chen X, Dewing P, Swain A, Rao PN, Elejalde BR, Vilain E 2001 Up-regulation of WNT4 signaling and dosage-sensitive sex reversal in humans. Am J Hum Genet 68:1102–1109
37. Mizusaki H, Kawabe K, Mukai T, Ariyoshi E, Kasahara M, Yoshioka H, Swain A, Morohashi K 2003 Dax-1 gene transcription is regulated by *Wnt4* in the female developing gonad. Mol Endocrinol 17:507–519
38. Brennan J, Capel B 2004 One tissue, two fates: molecular genetic events that underlie testis versus ovary development. Nat Genet Rev 5:509–521
39. Flejter W, Fergestad J, Gorski J, Varvill T, Chandrasekharappa S 1998 A gene involved in XY sex reversal is located on chromosome 9, distal to marker D9S1779. Am J Hum Genet 63:794–802
40. Raymond CS, Kettlewell JR, Hirsch B, Bardwell VJ, Zarkower D 1999 Expression of *Dmrt1* in the genital ridge of mouse and chicken embryos suggests a role in vertebrate sexual development. Dev Biol 215:208–220
41. Nanda I, Shan Z, Schartl M, Burt D, Koehler M, Nothwang H, Grutzner F, Paton I, Windsor D, Dunn I, Engel W, Staeheli P, Mizuno S, Haaf T, Schmid M 1999 300 million years of conserved synteny between chicken Z and human chromosome 9. Nat Genet 21:258–259
42. Matsuda M, Nagahama Y, Shinomiya A, Sato T, Matsuda C, Kobayashi T, Morrey C, Shibata N, Asakawa S, Shimizu N, Hori H, Hamaguchi S, Sakaizumi M 2002 DMY is a Y-specific DM-domain gene required for male development in the medaka fish. Nature 417:559–563
43. Vidal VPI, Chaboissier MC, de Rooij DG, Schedl A 2001 Sox9 induces testis development in XX transgenic mice. Nat Genet 28:216–217
44. De Santa Barbara P, Bonneaud N, Boizet B, Desclozeaux M, Moniot B, Sudbeck P, Scherer G, Poulat G, Berta P 1998 Direct interaction of SRY-related protein SOX9 and steroidogenic factor 1 regulates transcription of the human anti-Müllerian hormone gene. Mol Cell Biol 18: 6653–6665
45. Arango NA, Lovell-Badge R, Behringer RR 1999 Targeted mutatgenesis of the endogenous mouse *Mis* gene promoter: in vivo definition of genetic pathways of vertebrate sexual development. Cell 99:409–419
46. Behringer RR, Cate RL, Froelick GJ, Palmiter RD, Brinster RL 1990 Abnormal sexual development in transgenic mice chronically expressing Müllerian-inhibiting substance. Nature 345:167–170
47. Baron D, Cocquet J, Xia X, Fellous M, Guiguen Y, Veitia RA 2004 An evolutionary and functional analysis of *FoxL2* in rainbow trout gonad differentiation. J Mol Endocrinol 33:705–715
48. Hudson QJ, Smith CA, Sinclair AH 2005 Aromatase inhibition reduces expression of *FoxL2* in the embryonic chicken ovary. Dev Dyn 233:1052–1055
49. Pannetier M, Fabre S, Batista F, Kocer A, Renault L, Jolivet G, Mandon-Pepin B, Cotinot C, Veitia R, Pailhoux E 2006 FoxL2 activates P450 aromatase gene expression: towards a better understanding of the early steps of mammalian ovarian development. J Mol Endocrinol 36:399–413
50. Wang DS, Kobayashi T, Zhou LY, Paul-Prasanth B, Ijiri S, Sakai F, Okubo K, Morohashi K, Nagahama Y 2007 FoxL2 upregulates aromatase gene transcription in a female-specific manner by binding to the promoter as well as interacting with Ad4 binding protein/steroidogenic factor 1. Mol Endocrinol 21:712–725
51. Ramsey M, Shoemaker C, Crews D, Gonadal expression of Sf1 and aromatase during sex determination in the red-eared slider turtle (*Trachemys scripta*), a reptile with temperature-dependent sex determination. Differentiation, in press
52. Kim Y, Capel B 2006 Balancing the bipotential gonad between alternative organ fates: a new perspective on an old problem. Dev Dyn 235:2292–2300
53. Carroll TJ, Park JS, Hayashi S, Majumdar A, McMahon AP 2005 Wnt9b plays a central role in the regulation of mesenchymal to epithelial transitions underlying organogenesis of the mammalian urogenital system. Dev Cell 9:283–292
54. Martineau J, Nordqvist K, Tilmann C, Lovell-Badge R, Capel B 1997 Male-specific cell migration into the developing gonad. Curr Biol 7:958–968
55. Brennan J, Karl J, Capel B 2002 Divergent vascular mechanisms downstream of Sry establish the arterial system in the XY gonad. Dev Biol 244:418–428
56. Parr BA, McMahon AP 1998 Sexually dimorphic development of the mammalian reproductive tract requires Wnt7a. Nature 395:707–710
57. Wibbels T, Wilson C, Crews D 1999 Müllerian duct development and regression in a turtle with temperature-dependent sex determination. J Herpetol 33:149–152
58. Hanley NA, Hagan DM, Clement-Jones M, Ball SG, Strachan T, Salas-Cortes L, McElreavey K, Lindsay S, Robson S, Bullen P, Ostrer H, Wilson DI 2000 *Sry*, *Sox9*, and *Dax1* expression patterns during human sex determination and gonadal development. Mech Dev 91:403–407
59. Bouma GJ, Albrecht KH, Washburn LL, Recknagel AK, Churchill GA, Eicher EM 2005 Gonadal sex reversal in mutant *Dax1* XY mice: a failure to upregulate *Sox9* in pre-Sertoli cells. Development 132:3045–3054

60. Quinn AE, Georges A, Sarre SD, Guarino F, Ezaz T, Graves JA 2007 Temperature sex reversal implies sex gene dosage in a reptile. Science 316:411
61. De Santa Barbara P, Moniot B, Poulat F, Berta P 2000 Expression and subcellular localization of SF1, SOX9, WT1 and AMH proteins during early human testicular development. Dev Dyn 217:293–298
62. Lasala C, Carre-Eusebe D, Picard J, Rey R 2004 Subcellular and molecular mechanisms regulating anti-Müllerian hormone gene expression in mammalian and non-mammalian species. DNA Cell Biol 23:572–585
63. Pfaff MW 2001 A new mathematical model for relative quantification in real-time RT-PCR. Nucleic Acids Res 29:2002–2007
64. Muller P, Janovjak H, Miserez A, Dobbie Z 2002 Processing of gene expression data generated by quantitative real-time PCR. Biotechniques [Erratum (2002) 33:514] 32:1372–1379
65. Simon P 2003 Q-Gene: processing quantitative real-time RT-PCR data. Bioinformatics 19:1439–1440

Molecular Endocrinology **is published monthly by The Endocrine Society (http://www.endo-society.org), the foremost professional society serving the endocrine community.**